Development of a Freckle Predictor *via* Rayleigh Number Method for Single-Crystal Nickel-Base Superalloy Castings

C. BECKERMANN, J.P. GU, and W.J. BOETTINGER

A Rayleigh number based criterion is developed for predicting the formation of freckles in Ni-base superalloy castings. This criterion relies on finding the maximum local Rayleigh number in the mush, where the ratio of the driving buoyancy force to the retarding frictional force is the largest. A critical Rayleigh number for freckle formation of approximately 0.25 is found from available experimental data on directional solidification of a Ni-base superalloy. If the Rayleigh number in a superalloy casting is below this critical value, freckles are not expected to form. Full numerical simulations of freckling in directional solidification of superalloys are conducted for a large variety of casting conditions, alloy compositions, and inclinations of the system with respect to gravity. For the vertical cases, the Rayleigh numbers at the starting points of the predicted freckles are in good agreement with the critical value established from the experiments. The simulations confirm that the same critical Rayleigh number applies to different superalloys. The simulations for inclined domains show that even a small amount of inclination (less than 10 deg) significantly lowers the critical Rayleigh number and moves the freckles to the sidewall of the casting, where the mushy zone has advanced the most relative to gravity. In application of the Rayleigh number criterion to complex-shaped superalloy castings, the absence of freckles near upper and lower boundaries and in sections of insufficient cross-sectional area or height needs to be taken into account as well. The criterion can be used to study the tradeoffs between different superalloy compositions, applied temperature gradients, and casting speeds. Additional experiments, in particular for other superalloys and for a range of inclinations, are desirable to confirm the critical Rayleigh numbers found in the present study.

I. INTRODUCTION

FRECKLES (or channel segregates) have been the subject of intense research efforts for about 30 years,[1,2] due to their importance as a defect in alloy casting and the interesting fluid-mechanical phenomena associated with their formation.[3] Freckles are chains of small equiaxed grains in an alloy otherwise solidified with a columnar structure. In particular, in directionally solidified single-crystal superalloy parts, freckles are generally a cause of rejection.

Solidification experiments with transparent model alloys and binary metallic alloys have shown that freckles are initiated by convective instabilities in the high-liquid-fraction region of the mushy zone near the primary dendrite tips (for a review, refer to Hellawell *et al.)*.[4] During upward directional solidification into a positive temperature gradient, the melt inside the mushy zone can become gravitationally unstable due to chemical segregation of alloy elements at the scale of the dendrite arms. Such microsegregation can cause the local melt density to decrease during solidification if light alloy elements are preferentially rejected into the melt (for a partition coefficient less than unity) or if heavy alloy elements are preferentially incorporated into the solid (for a partition coefficient greater than unity). If the melt overcomes the retarding frictional force in the porous-medium-like mushy zone, convection cells form. Since the mass diffusivity of the liquid is much lower than its heat diffusivity, the segregated melt retains its composition as it flows upward through the mush into regions of higher temperature. There, the melt causes delayed growth and localized remelting of solid, such that pencil-shaped channels, devoid of solid, form in the mushy zone. Low-density, highly segregated liquid emanates from the channels as solutal plumes or fingers flowing upward into the superheated liquid. Hence, the channels provide self-sustaining paths for feeding the plumes. At the lateral boundary of the channels, higher-order dendrite arms can become detached from the main trunk, most likely by a local remelting process. These dendrite fragments either (1) remain in the channels and grow into the equiaxed grains later observed as freckle chains or (2) are advected out of the channels by the flow and, if not remelted completely, may form spurious grains inside the columnar structure or even cause a columnar-to-equiaxed transition.[1,4–6]

Clearly, the onset of freckling depends on the complicated interplay of the stabilizing thermal gradient (G); the speed of the isotherms (R) relative to the flow velocities; the structure and permeability of the mush, which, in turn, depend on the casting conditions G and R as well as on the variation of the solid fraction in the mush; the variation of the liquid density in the mush and, thus, the segregation behavior of the solutes as a function of the alloy composition and solidification path; and the casting geometry and growth direction relative to gravity. Copley *et al.*[7] suggested a criterion for

C. BECKERMANN, Professor, is with the Department of Mechanical Engineering, The University of Iowa, Iowa City, IA 52242-1527. J.P. GU, formerly Postdoctoral Researcher, Department of Mechanical Engineering, The University of Iowa, is Engineer with PCC Structurals Inc., Portland, OR 97206-0898. W.J. BOETTINGER, Metallurgist, is with the Metallurgy Division, National Institute of Standards and Technology, Gaithersburg, MD 20899.

Manuscript submitted January 25, 2000.

freckle formation that is based on a critical cooling rate ($\dot{T}$, equal to $G \times R$), below which freckles are likely to form. Their directional solidification experiments with the transparent analog system NH_4Cl-H_2O also showed that freckles appear preferentially at those locations of the casting cross section where the interface between the mushy zone and the overlying liquid region is the highest in the direction of gravity. This explains why freckles usually appear on the outside casting surface, instead of the interior, because, in most directional solidification processes, a small amount of lateral cooling will cause the mush/liquid interface to be concave. Detailed experimental work on freckling has also been carried out using Pb-Sn systems.[8–13] Pollock and Murphy[5] and Auburtin *et al.*[14] performed directional solidification experiments using Ni-base superalloys. The former investigators found a strong correlation between the primary dendrite arm spacing (λ_1) and freckle initiation, and, for one superalloy, the critical spacing above which freckles form was found to be 320 μm. Since, according to traditional theoretical models, λ_1 varies with $G^{-1/2} \times R^{-1/4}$,[15] they suggested this thermal parameter as an improved freckle criterion. However, for superalloys, the primary spacing has been experimentally found to be well correlated also by $\dot{T}^{-1/3}$,[16,17] lending support to the cooling rate based criterion of Copley *et al.*[7] as well. Due to the difficulty of performing such experiments over large ranges of G and R, the relative merits of the various thermal criteria are sometimes difficult to assess. Auburtin *et al.*[14] noted that a minimum cross-sectional area is required in order to support the fluid flow patterns associated with freckles. Since typical freckle spacings observed in experiments are about 5 to 10 mm, a minimum area for freckle formation of 25 to 100 mm^2 was estimated, which is supported by their experiments.

Several investigators have attempted to interpret their experimental results in terms of a nondimensional mushy zone Rayleigh number.[9,13,14,18] The Rayleigh number measures the ratio of the driving buoyancy force to the retarding frictional force associated with the permeability of the mush The main advantage of a Rayleigh number based criterion for freckle initiation over the aforementioned purely thermal criteria is that the influence of alloy composition is taken into account. In other words, the same critical Rayleigh number should apply to different alloy compositions. Unfortunately, the permeability variation in the mush is difficult to evaluate, thermophysical properties may not be known accurately, and every investigator appears to be using different definitions of the Rayleigh number. Therefore, a reliable value of the critical Rayleigh number for freckle initiation is still lacking.

Considerable progress in understanding the formation of freckles has been made by various theoretical analyses of convection in mushy layers, as reviewed by Worster.[3] Linear stability analyses[19–21] have been conducted to identify the critical Rayleigh number for which the system becomes unstable to infinitesimal disturbances. The nonlinear theories[22,23] confirm that the bifurcation to convection (and freckling) in mushy layers is subcritical, determine the global critical Rayleigh number below which the system is completely stable to disturbances of arbitrary amplitude, and show the various convection modes possible as a function of the Rayleigh number. The studies also reveal that the global critical Rayleigh number varies with at least four other system parameters, namely, the Stefan number, a dimensionless melt superheat, a dimensionless concentration ratio characterizing the phase diagram, and a parameter that describes the variation of the permeability with the solid volume fraction. The analyses are limited to steady directional solidification and a somewhat "ideal" mathematical model of the mushy layer.[3] Therefore, quantitative comparisons with actual laboratory experiments are discouraged,[23] and the application to casting of Ni-base superalloys is difficult.

Numerical simulations of the transport phenomena during alloy solidification, using the full set of conservation equations, also succeeded in predicting freckles beginning in the late 1980s.[24] Beckermann and Wang[25] and Prescott and Incropera[26] have reviewed this subject in detail. Although the numerical predictions appear qualitatively correct, the predictions for freckle initiation in directional solidification have never been compared to experiments and stability analyses. Furthermore, because such simulations are computationally expensive, they have not been used to fully explore the dependency of freckle initiation on the various system parameters. For the same reason, it will probably take many years before commercially available casting simulation codes can be used to directly simulate the formation of freckles in complex-shaped parts. With respect to directional solidification of Ni-base superalloys, Schneider *et al.*[27] developed a micro/macrosegregation model that is linked to a multicomponent thermodynamic phase equilibrium subroutine.[28] Two-dimensional simulation results are presented that investigate freckle formation for various thermal conditions and superalloy compositions, but, again, no direct comparisons with experiments or theories are made. More recently, Felicelli *et al.*[29] simulated freckling in three dimensions for a Ni-Al-Ta-W alloy.

The objective of the present study is to develop a Rayleigh number based criterion for freckle formation in Ni-base superalloy directional solidification, by using both available experimental data[5] and the results of full numerical simulations.[27] The experimental data serve to establish the basic validity of such a criterion and to evaluate the critical Rayleigh number for freckle initiation for one alloy composition and a certain set of experimental conditions. Because of the limited availability of experimental data, numerical simulations are then used to evaluate the critical Rayleigh number for other alloy compositions and casting conditions. The most interesting question here is whether the critical Rayleigh number deduced from the experiments agrees with the one from the full numerical simulations. For this purpose, the input parameters for the simulations are chosen to be reasonably close to typical single-crystal superalloy casting conditions. Then, any variation of the critical Rayleigh number with other system parameters (such as the dimensionless melt superheat discussed previously)[3] is minimized. Second, there are no ambiguities associated with the evaluation of the critical Rayleigh number from the simulation results, other than those related to the identification of the onset of freckling itself. When evaluating a Rayleigh number in experiments, considerable uncertainties exist in the mushy zone permeability variation, the thermal conditions, the liquid density variation in the mush, and other properties. These

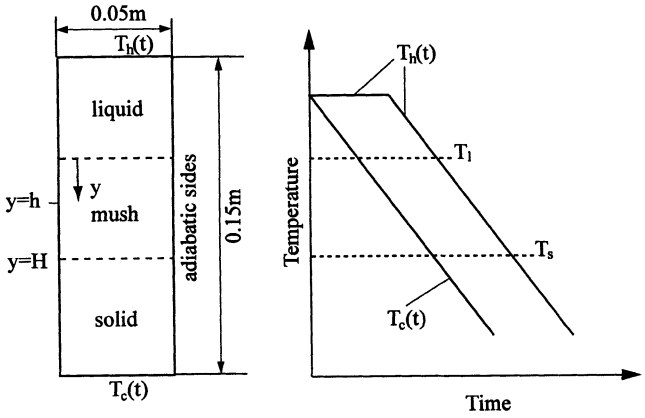

Fig. 1—Schematic of the directional solidification system and boundary conditions used in the numerical simulations.

parameters are all known in simulations. Self-consistent critical Rayleigh numbers can, thus, be obtained. Third, simulations allow for the investigation of a large range of alloy compositions and casting conditions. As part of the present study, extensive simulations are conducted to investigate the onset of freckling in domains that are inclined with respect to gravity. A brief discussion of the use and limitations of the proposed Rayleigh number criterion in predicting freckle formation for realistically shaped castings concludes the present study.

II. RAYLEIGH NUMBER

A. *Definition and Supplementary Relations*

Many different mushy zone Rayleigh number definitions have been proposed in the literature for characterizing freckle formation.[9,13,14,18,21,23] We have examined each one of them and found a definition similar to the one proposed by Worster[21] to be physically most meaningful:

$$\mathrm{Ra}_h = \frac{(\Delta\rho/\rho_0) g \overline{K}\, h}{\alpha\nu} \qquad [1]$$

The subscript h to the Rayleigh number (Ra) denotes that it is a mean value over a height h of the mushy zone, measured downward from the interface between the single-phase liquid and mushy regions (*i.e.*, from the primary dendrite tips). Figure 1 illustrates the directional solidification system considered in the present study. The height h varies from 0 to H, the total height of the mushy zone. For a given temperature gradient G, the height, h, is related to the local temperature, T, by $h = (T_l - T)/G$, where T_l is the liquidus temperature. Other symbols in Eq. [1] include the thermal diffusivity (α), the kinematic viscosity (ν) of the melt in the mush, and the gravitational acceleration (g, equal to 9.81 m/s^2). An approximate value of $\alpha\nu = 5 \times 10^{-12}$ m^4/s^2[30] is used throughout this study in evaluating the Rayleigh number.

The relative liquid density inversion ($\Delta\rho/\rho_0$) over the mush of height h is given by

$$\Delta\rho/\rho_0 = (\rho_0 - \rho(h))/\rho_0 \qquad [2]$$

where ρ_0 is the liquid density at the mush/liquid interface, $y = 0$ (evaluated at the liquidus temperature and solute concentrations corresponding to the nominal alloy composition), and $\rho(h)$ is the liquid density at $y = h$ (evaluated at the local temperature and liquid concentrations in the mush). The calculation of the liquid densities is described subsequently.

The mean permeability ($\overline{K}$) corresponding to the average solid fraction ($\overline{\varepsilon}_s$) in the mush of height h is calculated from

$$\overline{K} = K_0 \frac{(1 - \overline{\varepsilon}_s)^3}{\overline{\varepsilon}_s^{\,2}} \qquad [3]$$

where $K_0 = 6 \times 10^{-4}\ \lambda_1^2$, in which λ_1 is the primary dendrite arm spacing. This permeability relation is the same as the one used in the numerical simulations of Schneider *et al.*[27] and is based on the isotropic Blake–Kozeny equation. The numerical value in the coefficient K_0 was obtained from a best fit of experimental (at intermediate solid fractions) and theoretical (at low solid fractions) permeability data for flow parallel and perpendicular to the primary dendrites, as summarized in the thesis of Bhat.[31] Figure 4 in Schneider *et al.*[27] shows the curve fit. The same permeability relation has been found to produce good agreement with macrosegregation measurements in other systems.[32] More complicated relations, which also take the anisotropic nature of the mushy zone into account, could be used,[29] but the uncertainties are large, especially in view of the fact that the primary dendrite arm spacing (or other microstructural parameters) is not known exactly in castings. More simple permeability relations, such as those used by Sarazin and Hellawell,[9] Anderson and Worster,[23] and Auburtin *et al.*,[14] may provide physically reasonable functional dependencies, but do not always give the correct magnitude of the permeability.

In Eq. [3], the average solid fraction is given by

$$\overline{\varepsilon}_s = \frac{1}{h} \int_0^h \varepsilon_s\, dy \qquad [4]$$

where y is measured downward from the interface between the single-phase liquid and mushy regions (Figure 1). The calculation of the solid fraction variation in the mush is also described subsequently. The use of an average solid fraction in Eq. [3], first proposed by Worster,[21] results in an estimate of a mean permeability of the mush over the height h. This mean permeability is then "compared" to the density inversion over the same mush height in the Rayleigh number. The use of a local permeability, either at $y = 0$[21] or at $y = h$, would not be possible when using the present permeability relation (because $K(y = 0) \to \infty$) or would be physically less meaningful. For the same reasons, the permeability is not averaged directly.

The primary dendrite arm spacing λ_1 is the single most important parameter in the permeability relation and, hence, in the Rayleigh number (*i.e.*, Ra $\sim \lambda_1^2$). As in Schneider *et al.*,[27] it is calculated using an expression that has been found to be applicable to a wide range of superalloys:[17]

$$\lambda_1 = 147\ \dot{T}^{-0.3384} = 147\ (G \times R)^{-0.3384} \qquad [5]$$

where $\dot{T}$ is in K/s and λ_1 is in microns. In accordance with traditional theoretical models,[15] Pollock and Murphy[5] suggested that $\lambda_1 \sim G^{-1/2}\ R^{-1/4}$ for the arm-spacing measurements in their experiments, but noted that the aforementioned cooling rate based relation works well too.

B. *Calculation of Solidification Path, Microsegregation, and Liquid Densities*

The remaining parameters needed in the evaluation of the Rayleigh number are (1) the solid fraction variation with temperature or distance in the mush and (2) the variation of the liquid density in the mush as a function of temperature and liquid concentrations (C_l^m), where the superscript m denotes the species. These quantities can be obtained through a detailed consideration of phase equilibrium and microsegregation during solidification of superalloys. The method used here is the same as described in Schneider *et al.*,[27] and only a brief overview is provided here.

The phase equilibrium is calculated using a subroutine developed by Boettinger *et al.*[28] for Ni-base superalloys. The subroutine is based on the CALPHAD method[33] and relies on the use of thermodynamic free energy functions for the relevant phases in the alloy. It establishes the relation

$$C_l^m \Rightarrow (T, C_{si}^m) \qquad [6]$$

where C_{si}^m are the interfacial species concentrations in the solid for each element. By using this subroutine, the temperature/concentration dependence of partition coefficients and liquidus slopes is automatically taken into account, and any superalloy composition can be input. The thermodynamic database used in Schneider *et al.*[27] and in the full numerical simulations shown subsequently, as well as in the evaluation of the Rayleigh numbers for these cases (for consistency), is considered preliminary. In the evaluation of the Rayleigh numbers for the experiments, as described in the next section, a more refined database is used. The reader is referred to Kattner *et al.*[34] for further discussion of the databases and their use.

The phase equilibrium subroutine is linked to a microsegregation model to calculate the solidification path, *i.e.*, $\varepsilon_s(T)$.[27,28] In the full numerical simulations of Schneider *et al.*,[27] this model also includes consideration of macrosegregation (which results in changes in the average composition in a volume element due to flow), back-diffusion in the solid, and temperature dependent species diffusion coefficients in the solid. In the evaluation of the Rayleigh numbers, we only use a standard Scheil analysis. Because, at the point of freckle initiation, the melt flow is either weak or nonexistent and the solid fraction is small (less than 20 pct), any differences between the Scheil analysis and the full numerical simulations have a negligible effect on the Rayleigh number. Figure 2 in Schneider *et al.* shows examples of solidification path calculations for the superalloy IN718.

The knowledge of the liquid concentrations and the solidification path allows for the determination of the variation of the liquid density in the mush. The following formula from Iida and Guthrie[35] is used to calculate the liquid density:

$$\rho^{-1} = \sum_m \frac{C_l^m}{\rho_{\text{ref}}^m + \Lambda^m (T - T_{\text{ref}}^m)} \qquad [7]$$

where ρ_{ref}^m and T_{ref}^m are reference densities and temperatures, respectively, for each element, and $\Lambda^m = \partial \rho^m / \partial T$. Values for these three properties for each element in a superalloy can be found in Iiada and Guthrie.[35] Figure 3 in Schneider *et al.*[27] shows an example of the variation of the liquid density with solid fraction, calculated using the previous procedure, for the superalloy CMSX2.

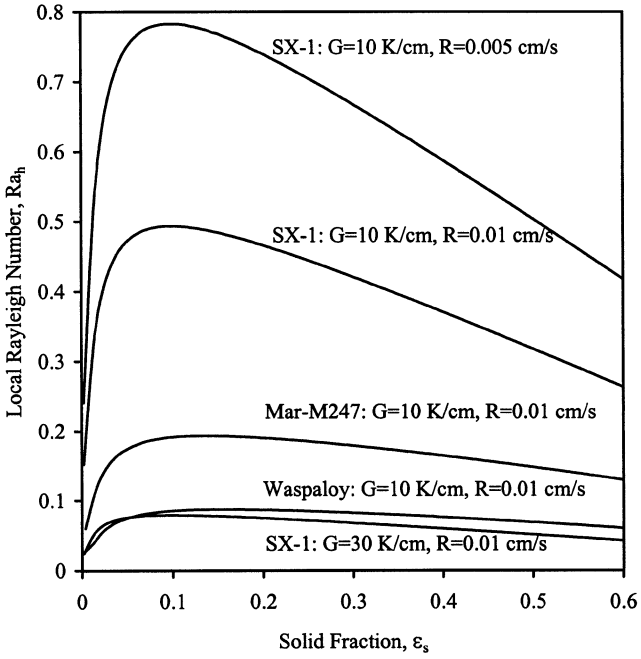

Fig. 2—Variation of the local mush Rayleigh number with solid fraction for three different Ni-base superalloys and several combinations of temperature gradient and growth speed.

C. *Maximum Rayleigh Number in the Mush*

Figure 2 shows the calculated variation of Ra_h with ε_s for the SX-1 superalloy of Pollock and Murphy[5] and the superalloys Waspaloy and Mar-M247, studied by Auburtin *et al.*[14] Their compositions are given in Table I. For these example cases, the Rayleigh number variation is plotted for several different combinations of G and R. It can be seen that for all alloys and thermal parameters, the Rayleigh number increases with solid fraction and reaches a maximum at around 10 to 15 pct solid. Beyond that solid fraction, the Rayleigh number decreases. A maximum exists because the density inversion increases with solid fraction, whereas the permeability decreases. The maximum Rayleigh number corresponds to the location in the mushy zone where the buoyancy force is the largest relative to the permeability drag. It is in this high-liquid-fraction region where channels are most likely to be initiated. Closer to the primary dendrite tips, the buoyancy forces are not large enough. Deeper inside the mush, the permeability is too small.

The maximum Rayleigh number, thus, serves as a physically meaningful, single reference value for evaluating stability to freckling. The maximum is also convenient, because it varies by less than 10 pct for solid fractions ranging from 5 to more than 20 pct. Choosing the Rayleigh number closer to $y = 0$, or deeper inside the mush, as a reference value would make it quite sensitive to the solid fraction variation. In the following text, this maximum Rayleigh number is simply denoted by Ra, *i.e.*,

$$\text{Ra} \equiv \text{Ra}_h \big|_{\max} \qquad [8]$$

Using average G and R values over the upper 20 pct of the mush (which corresponds to a temperature range of about 10 K below the liquidus temperature for most superalloys)

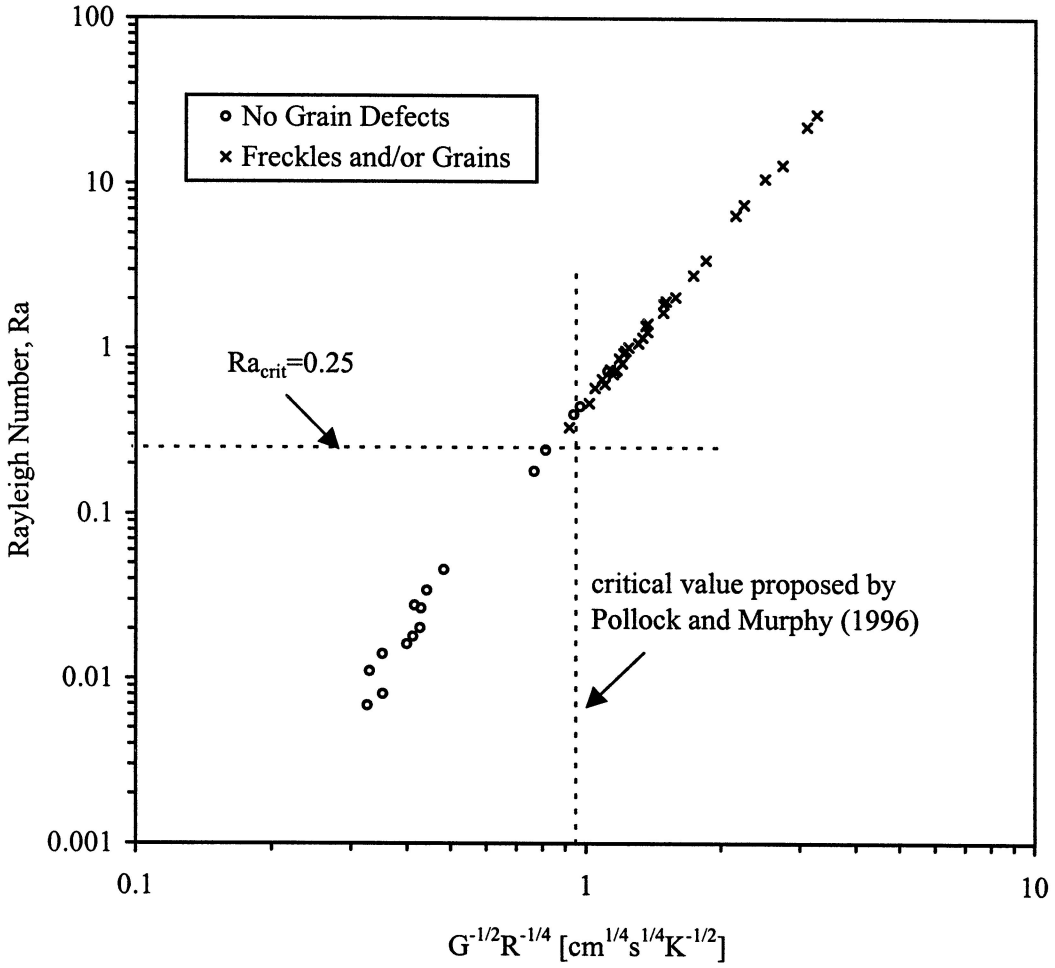

Fig. 3—Calculated Rayleigh numbers for the directional solidification experiments of Pollock and Murphy[5] for the SX-1 superalloy as a function of the thermal parameter $G^{-1/2} \times R^{-1/4}$, and establishment of the critical Rayleigh number based on the grain defect measurements.

Table I. Superalloy Compositions in Weight Percent (Excluding Small Amounts of Hf)

Alloy	Al	Cr	Co	Re	Ti	Ta	Mo	W	Ni
SX-1	6.0	4.5	12.5	6.3	—	7.0	—	5.8	bal
Waspaloy	1.2	19.0	12.3	—	3.0	—	3.8	—	bal
Mar-M247	5.5	8.5	10.0	—	1.0	3.0	0.6	10.0	bal
CMSX2	5.6	8.0	5.0	—	1.0	6.0	0.6	8.0	bal
CMSX2m	5.6	8.0	5.0	—	1.0	1.0	0.6	13.0	bal

should be most appropriate in evaluating the maximum Rayleigh number from experiments or casting simulations. Once the maximum Rayleigh number is found, it needs to be compared to some critical value (Ra_{crit}) to judge the stability to freckling. Here, the critical Rayleigh number is defined such that freckles will not form if

$$Ra < Ra_{crit} \quad [9]$$

The following sections are devoted to determining the critical Rayleigh number from experiments and numerical simulations, including consideration of the effect of inclination of the directional solidification system with respect to gravity. This critical value should be the same for all superalloys, assuming a minimal variation with other system parameters (as discussed in Section I). It should be emphasized, however, that the critical value would depend strongly on the definition of the Rayleigh number. If a definition different from the one proposed here is used, or if a different permeability relation is used, the critical value will change. Note that Eq. [9] does not imply that there will always be freckles if $Ra > Ra_{crit}$. As reviewed by Worster,[3] it is possible for the system to be stable above the global critical Rayleigh number if the disturbances are not of a sufficient magnitude. Other reasons could be that the casting cross section or the section height is not sufficient to support freckles (refer to Section I).

The usefulness of the present Rayleigh number criterion can be understood by comparing the maximum Rayleigh numbers for the SX-1, Mar-M247, and Waspaloy alloys in Figure 2. For the same thermal parameters (G = 10 K/cm and R = 0.01 cm/s), the maximum Rayleigh numbers for these three alloys are approximately 0.5, 0.2, and 0.09, respectively. Hence, the Waspaloy alloy is more than 5 times as stable (in terms of the Rayleigh number) as the SX-1 alloy and more than twice as stable as the Mar-M247 alloy, for the same casting conditions. A freckle criterion based solely on thermal parameters would not be able to distinguish

these differences in stability between the three alloys. It can also be seen from Figure 2 that for $R = 0.01$ cm/s, the Waspaloy alloy has about the same maximum Rayleigh number at $G = 10$ K/cm as the SX-1 alloy at $G = 30$ K/cm. Other illustrative examples can be found.

Before leaving this section, it is useful to examine how the maximum Rayleigh number varies with the thermal parameters G and R for a given alloy. Since $K \sim \lambda_1^2 \sim \dot{T}^{-2/3}$ (Eqs. [3] and [5]), $h \sim G^{-1}$ (refer to the paragraph below Eq. [1]), and the properties are approximately constant for a given alloy, the definition of the Rayleigh number (Eq. [1]) gives

$$\mathrm{Ra} \sim \dot{T}^{-2/3}\, G^{-1} = R^{-2/3}\, G^{-5/3} \qquad [10]$$

It can be easily verified from Figure 2 that this proportionality is true. Hence, the Rayleigh number criterion (Eq. [9]) can be expressed for a given alloy in terms of thermal parameters as

$$R^{-2/3} G^{-5/3} < \text{constant} \qquad \text{or, equivalently,} \qquad [11]$$
$$G^{-1/2}\, R^{-1/5} < \text{constant}$$

where the constants are different. The latter inequality in Eq. [11] is quite similar to the thermal criterion proposed by Pollock and Murphy,[5] *i.e.*, $G^{-1/2} \times R^{-1/4} <$ constant. While this approximate correspondence lends some confidence to the present Rayleigh number criterion, it should be emphasized again that such thermal criteria work only for a given alloy, because the constants would be different for every alloy composition.

III. EVALUATION OF THE CRITICAL RAYLEIGH NUMBER FROM EXPERIMENTS OF POLLOCK AND MURPHY[5]

Pollock and Murphy[5] conducted a series of directional solidification experiments on the SX-1 superalloy (Table I), where they systematically varied the casting conditions. Single crystals were vertically cast in the form of cylindrical bars, rectangular slabs, and solid blade-shaped samples. For all experiments, the primary dendrite arm spacing λ_1 and the withdrawal rate R were measured directly. In a few selected experiments with blade-type samples, the thermal gradient G was measured indirectly by insertion of thermocouples. The thermal gradient was then calculated by dividing the measured cooling rate between the liquidus and solidus temperatures by the withdrawal rate. For most of those samples, the arm spacings calculated from Eq. [5] agreed reasonably well with the measured spacings. However, because the thermal conditions were rather complex in the blade-type samples and the thermal gradient in the Rayleigh number is defined differently, the indirectly measured thermal gradients are not used in the present study. Instead, all thermal gradients are calculated from Eq. [5] using the measured arm spacings and withdrawal rates.

For each experiment, Pollock and Murphy counted the number of freckle chains and isolated, highly misoriented (or spurious) grains. In all but a few experiments, spurious grains were observed whenever freckles were present. The mechanisms for spurious grain formation in the presence of freckling are discussed in more detail in Gu *et al.*[6] (refer also to Section I). We obtained the original data from Pollock and Murphy and calculated the Rayleigh number corresponding to each experiment using the measured dendrite arm spacings and withdrawal rates, as discussed previously. Figure 3 shows the Rayleigh numbers as a function of $G^{-1/2} \times R^{-1/4}$. The occurrence of freckles and/or spurious grains is indicated in the figure, using different symbols. It can be seen that the transition to freckling is well correlated by both the Rayleigh number and the thermal criterion of Pollock and Murphy, who proposed $G^{-1/2} \times R^{-1/4} < 0.95$ cm$^{1/4}$ s$^{1/4}$ K$^{-1/2}$ as the critical value for the SX-1 alloy. This correspondence is not surprising, as explained in the previous section. Around the critical value, there is some scatter in the data, which is well within the experimental uncertainties.

As can be seen from Figure 3, the critical Rayleigh number corresponding to the transition value proposed by Pollock and Murphy is approximately $\mathrm{Ra}_{\mathrm{crit}} = 0.4$. Considering the spread of the data and the uncertainties in the thermal parameters, a more conservative critical Rayleigh number as low as $\mathrm{Ra}_{\mathrm{crit}} = 0.25$ is possible as well. This seemingly large uncertainty in the critical Rayleigh number is caused by the fact that the Rayleigh number is more sensitive to variations in G and R (Eq. [10]) than the thermal criterion $G^{-1/2} \times R^{-1/4}$. In practice, it simply means that uncertainties in the thermophysical properties and permeability relation used in the calculation of the Rayleigh number are less important than variations in the thermal parameters. Clearly, additional experimental data around the critical value, and for different superalloys, would be highly desirable to further validate the proposed Rayleigh number criterion.

IV. EVALUATION OF THE CRITICAL RAYLEIGH NUMBER FROM SIMULATIONS

The recently developed numerical simulation model of Schneider *et al.*[27] is used in this section to predict the onset of freckling in directional solidification of Ni-base superalloys. The main objective is to determine a value for the critical Rayleigh number from the simulations. A comparison with the value determined in the previous section from experiments will then validate the simulations. The simulations are conducted for superalloys different from the SX-1 alloy, in order to test the concept of a single critical Rayleigh number for all superalloys. Additional simulations are conducted to determine critical Rayleigh numbers for domains that are inclined relative to gravity.

A. *Description of the Numerical Simulations*

The numerical simulations of directional solidification of single-crystal, Ni-base superalloys were conducted using the model, system, and properties of Schneider *et al.*[27] As discussed in the Introduction, the micro/macrosegregation model consists of fully coupled mass, momentum, energy, and species conservation equations for solidification together with a phase equilibrium subroutine for multicomponent Ni-base superalloys. The system is illustrated in Figure 1 and consists of a two-dimensional rectangular cavity of height and width equal to 0.15 and 0.05 m, respectively. The sidewalls are adiabatic, while the top and bottom walls are maintained at time-varying hot (T_h) and cold (T_c) temperatures, respectively, as shown in Figure 1, such that solidification proceeds directionally from the bottom toward the top

Table II. Summary of Simulation Cases for the CMSX2 and CMSX2m Superalloys

Case	Inclination (Deg)	$(T_h - T_c)/15$ (K/cm)	$dT_{c,h}/dt$ (K/hr)	λ_1* (μm)	Freckle Start** (cm)	Rayleigh Number†
1-0	0	50	1250	210	no freckle	—
2-0	0	35	350	320	12.5	—§
3-0	0	30	300	340	8.5 ± 1	0.239
4-0	0	20	200	400	4.5 ± 1	0.175
6-0	0	12	120	463	0.8	0.208
1m-0‡	0	50	1250	210	11.5 ± 1	0.250
3m-0	0	30	300	340	3.0	0.229
4m-0	0	20	200	400	0.8	0.288
1-10	10	50	1250	210	12.9	—§
1.5-10	10	50	500	286	7.5	0.086
2-10	10	35	350	320	5.7	0.096
3-10	10	30	300	340	5.0	0.108
4-10	10	20	200	400	2.3	0.123
5-10	10	16	160	420	1.0	0.140
1-30	30	50	1250	210	11.3	0.079
1.5-30	30	50	500	286	7.1	0.080
2-30	30	35	350	320	4.7	0.082
4-30	30	20	200	400	1.0	0.102
1-45	45	50	1250	210	9.7	0.042
1.5-45	45	50	500	286	5.4	0.057
2-45	45	35	350	320	4.2	0.076
3-45	45	30	300	340	2.0	0.069

*Primary dendrite arm spacing is assumed constant for each simulation.

**Distance of the freckle starting point from the bottom; the uncertainty is ±0.5 cm unless otherwise indicated.

†Rayleigh number based on the local temperature gradient at the freckle starting point.

‡The term *m* refers to the modified CMSX2m composition.

§No reliable value of the Rayleigh could be computed for these cases because the variation of the temperature gradient near the top wall was too large.

wall. Different solidification conditions are achieved by varying the global cooling rate ($dT_c/dt = dT_h/dt$) and temperature gradient ($(T_h - T_c)/0.15$ m), where t denotes time. The top wall is maintained at the initial temperature, equal to the liquidus temperature of the alloy plus 150 K superheat, until the bottom wall reaches a temperature consistent with the desired global temperature gradient. Note that these conditions are applied at the top and bottom boundaries. The cooling rates and temperature gradients inside the domain are a consequence of the solution of the energy equation and depend on location and time. The primary dendrite arm spacing was assumed constant for each simulation and was calculated from Eq. [5] using the global cooling rate. In the simulations for an inclined domain, only the gravity vector in the momentum equations was changed.

As in Schneider *et al.*,[27] simulations are reported for the superalloy CMSX2 and a modified CMSX2 alloy, denoted by CMSX2m, whose compositions are listed in Table I. The modification of the CMSX2 alloy consists of decreasing Ta from 6 to 1 wt pct and increasing W from 8 to 13 wt pct, resulting in a considerably more unstable alloy. Recall from Section II–B that all simulations of this section are performed using a preliminary thermodynamic database for Ni-base superalloys, as described in Schneider *et al.*[27] Therefore, the two alloys can be regarded as somewhat hypothetical (for example, the solidification interval is too large), but, since the Rayleigh number is evaluated using the same thermodynamic database, consistent results are obtained. All other properties used in the simulations are listed in Schneider *et al.*

The simulation cases are listed in Table II. Only six of the 22 simulations were already reported in Schneider *et al.*,[27] and all simulations for an inclined domain are new. Figure 4 shows an example of simulation results for a vertical domain (case 4m-0) and Figure 5 for a domain inclined at 30 deg (case 2-30). The results are for some intermediate time during solidification, when the mush/liquid interface has advanced a little further than midheight and a thin, fully solid layer appeared at the bottom. The left-hand-side panels show the isotherms (equal intervals); the middle panels show the liquid velocities and solid fraction contours (equal intervals of 20 pct); and the right-hand-side panels show the mixture concentration (equal intervals between the gray shades) of Ti, normalized by the initial concentration (the patterns being similar, if scaled, for the other elements). Noteworthy are the long channels in the mush, devoid of solid, through which the segregated liquid flows upward to feed a plume above the channel in the single-phase liquid region. These channels lead to freckle chains, as described in the Introduction. For the vertical case (Figure 4), several channels initially compete for the available horizontal space. Eventually, three channels, one at each sidewall and one in the middle, survive. The freckle spacing and sizes are similar to what is observed in experiments.[4]

For the inclined case (Figure 5), only one channel is predicted along the upper sidewall. The one channel exists at that location because low density, segregated liquid flows upward inside the mush and accumulates along the upper sidewall. This accumulation, which occurs even before channel formation, can be observed in Figure 5 as a band of increased solute concentration (for Ti) along the upper sidewall and preceding the open channel. The channel itself is

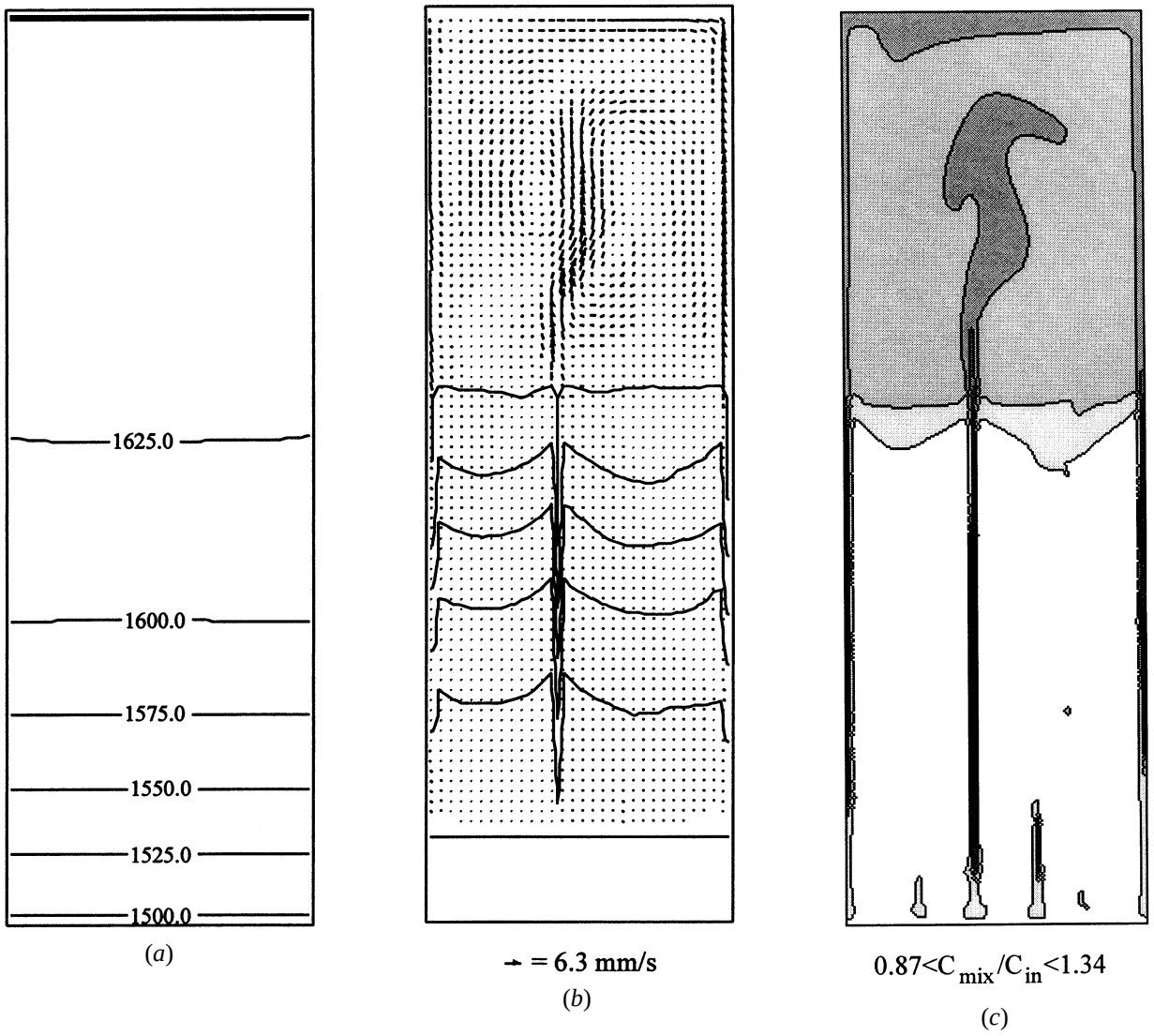

Fig. 4—Example simulation results for a vertical domain (case 4m-0): (*a*) isotherms in Kelvin, (*b*) velocity vectors and solid fraction contours (in 20 pct increments), and (*c*) normalized mixture concentration pattern of Ti.

somewhat thinner and characterized by a much higher solute concentration (for Ti). The low density liquid coming out of the channel flows along the upper sidewall toward the top boundary.

Another consequence of the inclination is the presence of a thermally driven, clockwise rotating convection cell in the single-phase liquid region. The liquid is cooled at the mush/liquid interface, flows toward the lower sidewall, and then flows upward along the lower sidewall. Along the upper sidewall, there exists a counterflow, with the channel plume flowing toward the top and the thermally driven cell toward the mush/liquid interface. Note in Figure 5 that the liquidus isotherm corresponding to the nominal alloy composition (1606 K) does not coincide with the mush/liquid interface. This can be explained by the thermally driven flow near the mush/liquid interface advecting solute from the upper regions of the mush into the single-phase liquid region. The segregated liquid has a lower liquidus temperature and, hence, delays solidification near the lower sidewall, in a manner similar to the liquid inside the channel. This advection of solute can be observed in the mixture-concentration plot of Figure 5, which shows considerable deviations from the nominal concentration in the upper mush and higher concentrations (of Ti) in the liquid along the lower sidewall.

Convection patterns similar to the inclined case are responsible for the observation that freckles appear preferentially at those locations of the casting cross section where the mushy zone has advanced the most (usually on the outside casting surface, where the cooling is the greatest).[7] The localization of freckles due to inclination can also be used to purposely move freckles to a location in the casting cross section that is later removed.

B. *Calculation of the Local Rayleigh Number in the Simulations*

Having accomplished the prediction of freckles for a range of global thermal conditions, alloy compositions, and inclinations (Table II), the next step is to determine the Rayleigh number in the simulations. The Rayleigh number varies in space and time during each simulation, because the domain

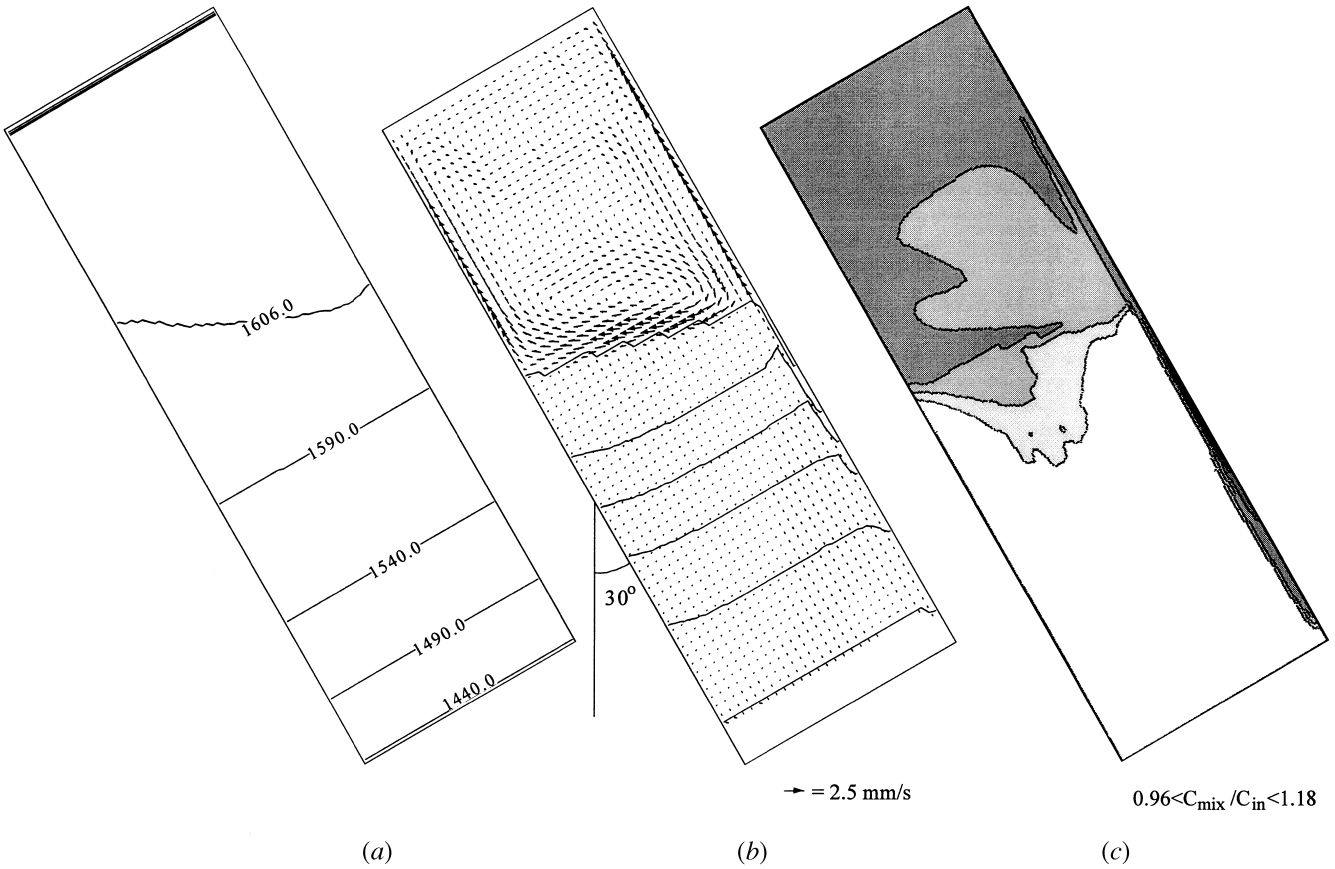

Fig. 5—Example simulation results for an inclined domain (case 2-30): (*a*) isotherms in Kelvin, (*b*) velocity vectors and solid fraction contours (in 20 pct increments), and (*c*) normalized mixture concentration pattern of Ti.

is not long enough for the heat transfer to become quasi-steady. This can be observed, for example, from the isotherms plotted in Figure 4(a), which indicate that the vertical temperature gradient is much higher near the cooled bottom wall than in the upper part of the cavity. Consequently, according to Eq. [10], the Rayleigh number can be expected to increase with height from the bottom of the domain. Since the primary dendrite arm spacing was assumed to be constant in each simulation case (at the values provided in Table II), variations in the cooling rate have no influence on the Rayleigh number. Thus, the knowledge of the temperature gradient alone, in addition to the alloy composition and the primary dendrite arm spacing, is sufficient to evaluate the local Rayleigh number in the simulations.

The following steps were taken in determining the variation with height from the bottom of the Rayleigh number in the simulations:

(1) Each simulation case was repeated with convection turned off. This has a negligible effect on the temperature gradients, because convection is nonexistent (in the vertical cases) or weak (in the inclined cases) *before* channel formation. In view of Table II, this meant seven different simulations for the CMSX2 alloy (cases 1, 1.5, 2, 3, 4, 5, and 6), and three simulations for the CMSX2m alloy (1m, 3m, and 4m). With the flow turned off, the inclination has no effect on the heat conduction simulation.
(2) The local temperature gradient was evaluated at each time step by measuring the distance h between the liquidus isotherm and the isotherm 10 K below liquidus; then, $G = 10\ \text{K}/h$. This gradient was assigned to the location midway between the two isotherms. A temperature interval of 10 K was chosen in order to obtain a mean gradient in the region of the mush where the Rayleigh number is maximum (Section II–C). When done, a smooth variation of the temperature gradient with height from the bottom is obtained.
(3) With the knowledge of the temperature gradient, alloy composition, and primary dendrite arm spacing, the (maximum) Rayleigh number is calculated at each height using the procedure detailed in Section II.

The resulting variation of the Rayleigh number with height from the bottom of the domain for each of the different simulation cases is shown in Figure 6. Because of the decrease of the temperature gradient with height from the bottom, the Rayleigh number increases for each case, as expected from Eq. [10]. At any particular height, the Rayleigh number increases when going from case 1 to 6, in accordance with the decrease in the applied global-temperature gradient (Table II). Comparing cases 1 with 1m, 3 with 3m, and 4 with 4m, it can be seen that the CMSX2 alloy is roughly 3 times more stable, in terms of the Rayleigh number, than the CMSX2m alloy for the same thermal conditions.

C. *Critical Rayleigh Number for Vertical and Inclined Simulation Cases*

In view of the strong variation of the Rayleigh number with height from the bottom of the domain during the simulations (Figure 6), the next step is to decide which Rayleigh

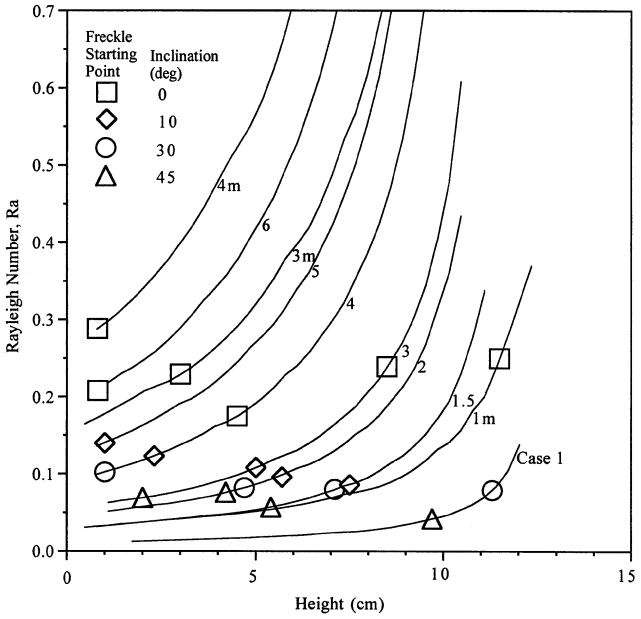

Fig. 6—Variation of the Rayleigh number in the simulations with height from the bottom of the domain (solid lines) and critical Rayleigh numbers corresponding to the predicted freckle starting points (symbols); results are shown for all vertical and inclined cases of Table II.

number is associated with freckle formation. Since Eq. [9] defines the critical Rayleigh number as the value below which freckles will *not* form, the Rayleigh number at the *starting* point of a freckle was chosen to be the critical value. The height of the starting point of a freckle is measured from the plots of the mixture concentration (of Ti), such as those shown in Figures 4(c) and 5(c). An open channel and, hence, a freckle is only associated with the darkest shade (*i.e.*, the strongest macrosegregation) in these plots. Each freckle is preceded by a trail of weaker macrosegregation, which does not correspond to an open channel in the mush. This is particularly evident in the inclined cases along the upper sidewall (Figure 5(c)), as explained in Section IV–A. Therefore, for the example of Figure 5(c), the freckle starting point is at a height of approximately 4.7 cm, not closer to the bottom wall where the weak macrosegregation trail starts. The uncertainty in the freckle starting point measurement is estimated to be ± 0.5 cm.

The freckle starting point measurements for each simulation case are listed in Table II, together with the values of the corresponding Rayleigh number. The freckle starting points are also included in Figure 6 as symbols on the curves of the Rayleigh number variation for each case. For example, three symbols are present on the curve for case 4, because three simulations (4-0, 4-10, and 4-30) were performed under those thermal conditions. Going horizontally to the left of each symbol, the critical Rayleigh number for each simulation case can be read off the figure. Note that an uncertainty of ± 0.5 cm in the freckle starting point location translates to an uncertainty of approximately 20 pct in the critical Rayleigh number.

Focusing first on the vertical cases, the following observations can be made. To within the present uncertainties, the critical Rayleigh numbers for all vertical cases, except case 4m-0, are the same, the mean value being $Ra_{crit} = 0.22$ (standard deviation: 0.03). This constancy in the critical Rayleigh number for the vertical cases is remarkable, considering the large range of thermal conditions, freckle starting point heights, and alloy compositions covered in the simulations. For example, the critical Rayleigh number for cases 3-0 and 6-0 (CMSX2 alloy) are the same to within the uncertainty, even though the freckle starting point is 8.5 cm in the former case and 0.8 cm in the latter. Similarly, the critical Rayleigh numbers for cases 3-0 and 3m-0 are the same, even though the CMSX2 alloy is about 3 times more stable than the CMSX2m alloy for the same thermal conditions (as discussed previously). The reason for the discrepancy in case 4m-0 can be explained by the fact that the freckle starting point is essentially at the bottom of the domain (Figure 4). Freckles will form at the bottom of the domain whenever the Rayleigh number is above the critical value. For case 4m-0, the Rayleigh number near the bottom is about 0.3, so freckles will form right away.

The critical Rayleigh number of 0.22 ± 0.03, determined from the simulations for vertical directional solidification, is in excellent agreement with the conservative value of 0.25 obtained in Section III from the experiments of Pollock and Murphy.[5] The agreement is remarkable, considering the uncertainties in evaluating for the experiments the permeability, thermal parameters, and, to a lesser extent, thermophysical properties. This comparison can, therefore, be regarded as a quantitative experimental validation of the numerical predictions of freckle formation. Clearly, more comparisons are desirable, but, considering the Rayleigh number range covered in both the experiments and simulations (from about 0.01 to more than 10 (Figures 3 and 6)), the evidence is strong. The good agreement between the critical Rayleigh numbers for the SX-1, CMSX2, and CMSX2m alloys also indicates that the concept of a single critical Rayleigh number for all superalloys is valid within the range of compositions and casting conditions studied.

For the inclined cases, the following observations can be made from Figure 6. The critical Rayleigh numbers for the inclined domains are below those for the vertical domain. Furthermore, the critical Rayleigh numbers decrease with increasing inclination angle. As for the vertical domain, the critical Rayleigh numbers are the same for each inclination to within the present uncertainty. The mean values for each inclination, together with their standard deviations, are plotted in Figure 7 to better illustrate these trends. The standard deviations are generally of the same magnitude as the uncertainty in determining the critical Rayleigh number (*i.e.*, 20 pct).

As indicated in Figure 7 by the dashed line, the decrease in the critical Rayleigh number with inclination can be represented by the following fit:

$$Ra_{crit} = 0.125 - 0.0014\phi \quad \text{for } 10 \text{ deg} \le \phi \le 45 \text{ deg} \qquad [12]$$

where ϕ is the inclination angle, in degrees, of the domain. Other fits, including one that involves trigonometric functions, could be found, but Eq. [12] adequately describes the present limited data. The decrease in the critical Rayleigh number with increasing inclination can be explained by the accumulation of segregated, buoyant liquid along the upper sidewall before freckle formation, as explained in connection with Figure 5 in Section IV–A. The larger the inclination,

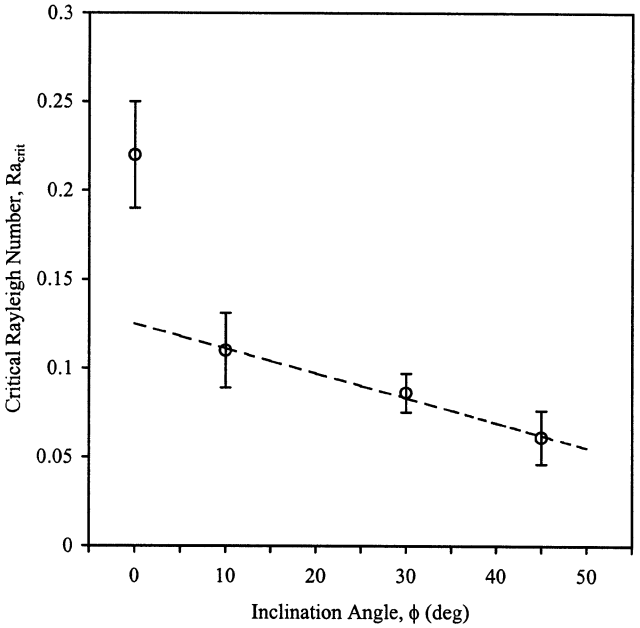

Fig. 7—Predicted critical Rayleigh number (symbols) as a function of the inclination angle of the domain; the uncertainty in the critical Rayleigh number, corresponding to ±1 standard deviation, is indicated by the vertical lines for each symbol; the interrupted line is a straight line fit of the critical Rayleigh numbers for the inclined cases.

the more segregated liquid flows toward the upper sidewall and contributes to the initiation of an open channel.

Interestingly, Figure 7 shows that an extension of the straight line through the critical Rayleigh numbers for the inclined cases, given by Eq. [12], does not meet the critical Rayleigh number at zero inclination. There is a difference of about a factor of 2 (0.125 *vs* 0.22), implying that there must be a sharp decrease in the critical Rayleigh number between 0 and 10 deg. Hence, even small inclinations (less than 10 deg) can significantly reduce stability to freckling. The sharp decrease may be explained by the qualitatively different convection patterns in the vertical and inclined cases. In the vertical case, there is no convection in the mush before channel initiation, and at least three channels compete for the same buoyancy (Figure 4). As soon as there is some inclination, segregated liquid flows toward the upper sidewall where the channel forms, and all of the available buoyancy contributes to only one channel (Figure 5). In directional solidification of complex-shaped parts, some inclination of the local temperature gradient with respect to gravity can be expected to be present always, and the value of the critical Rayleigh number for the vertical case (0.25) may never be applicable for those parts. The good agreement of the critical Rayleigh number for the vertical case with the experiments of Pollock and Murphy[5] indicates that the inclination effect was small in the experiments. However, the scatter in the experimental data around the critical value (Figure 3) may be partially due the various sample geometries and furnaces used by Pollock and Murphy resulting in different inclination effects. Only direct simulations of each experiment, together with a careful evaluation of the local temperature gradients and growth directions, can clarify this issue. Certainly, additional experiments with a range of sample inclinations are needed to validate the present simulation results for the inclined cases.

V. APPLICATION TO CASTING

The proposed Rayleigh number criterion can provide a simple means of evaluating stability to freckling in casting of single-crystal Ni-base superalloys. The first step would be to determine the local temperature gradients and cooling rates in the casting during solidification. This can be accomplished experimentally through the use of multiple thermocouples inside the casting, or numerically through the use of well established casting simulation codes. Since the heat transfer in complex-shaped castings is rarely quasi-steady, care should be taken to evaluate the thermal conditions in all parts of the casting, at the correct times, and over an appropriate temperature interval, in a manner consistent with the definition of the present Rayleigh number. When using simulation, it is also straightforward to determine the local inclination of the temperature gradient with respect to gravity. In experiments, it is desirable to measure the primary dendrite arm spacing directly, instead of calculating it from a correlation such as Eq. [5]. Then, the local (maximum) Rayleigh number can be calculated according to the procedure detailed in Section II. Here, the most difficult part is the evaluation of the liquid densities during solidification. This can typically only be accomplished if thermodynamic software, such as the one used in the present study, or detailed phase equilibrium information (*i.e.*, liquidus slopes and partition coefficients) are available, which allow for the calculation of the liquid species concentrations for a certain solidification path (*e.g.*, Scheil analysis, Section II–B). Fortunately, such software is rapidly becoming generally available. Finally, the calculated map of Rayleigh numbers should be compared to the critical Rayleigh number established in the present study. Since the numerically determined effect of inclination on the critical Rayleigh number has not yet been verified experimentally, caution should be exercised when using Eq. [12]. Nonetheless, critical Rayleigh numbers significantly below 0.25 can be expected when the temperature gradient is not vertical, such as in the presence of multidirectional cooling or cross-sectional changes.

There are several additional items that should be taken into account when interpreting the calculated Rayleigh number map for a casting.

(1) Although the critical Rayleigh number is associated with the starting point of a freckle in the full numerical simulations, the Rayleigh number criterion cannot provide the exact location and number of freckles in a casting cross section (*i.e.*, in a plane normal to the temperature gradient). Furthermore, the Rayleigh number criterion cannot be used to accurately determine the end point of freckles, because freckles can be expected to persist for some distance even if the local Rayleigh number falls significantly below the critical value after initiation.
(2) Even if the Rayleigh number is well above the critical value, freckles may not form if the casting cross section is too small. As noted in the Introduction, a minimum cross-sectional area is required to support the fluid flow patterns associated with each freckle, specifically, the downward flow through the mush to feed the open channel. This area is estimated to be of the order of 25 to 100 mm^2,[14] but further study is required.
(3) Similarly, a freckle will not form, regardless of the calculated Rayleigh number, if insufficient vertical height is available in the casting to support the fluid flow patterns

associated with a freckle. Above a wall, it is estimated that at least 20 pct of the total thickness of the mushy zone must be present before freckles can form. This estimate is supported by the fact that freckles start several millimeters away from a lower boundary, depending on the temperature gradient. A similar estimate can be made for the necessary height of the single-phase liquid region above the mush, and freckles will end a few millimeters before the mush reaches an upper boundary. As a consequence, freckles will not exist inside the relatively thin platforms typical in turbine blade castings.

VI. CONCLUSIONS

A Rayleigh number based criterion has been developed for predicting the formation of freckles in Ni-base superalloy castings. This criterion relies on finding the maximum local Rayleigh number in the mush, where the ratio of the driving buoyancy force to the retarding frictional force is the largest. A critical Rayleigh number for freckle formation of approximately 0.25 has been established using the experimental data on directional solidification of a Ni-base superalloy of Pollock and Murphy.[5] If the local (maximum) Rayleigh number in a superalloy casting is below this critical value, freckles are not expected to form. Additional experiments, in particular, for other superalloys and casting configurations, are desirable to confirm the critical value. Such experiments should be accompanied by numerical simulation of the heat transfer during casting, in order to establish accurately the local thermal conditions.

Full numerical simulations of freckling in directional solidification of superalloys have been conducted for a large variety of casting conditions, alloy compositions, and inclinations of the system. For the vertical cases, the Rayleigh numbers at the starting points of the predicted freckles are in good agreement with the critical value established from the experiments. Although additional comparisons should be performed, the agreement represents a first experimental validation of freckle predictions from full numerical simulations. The simulations also confirm that the same critical Rayleigh number applies to different superalloys, within the parametric ranges studied. This implies that the Rayleigh number based criterion can be used to study the tradeoffs between different superalloy compositions, applied temperature gradients, and casting speeds.

Additional simulations provide a first insight into the effect of inclination of the casting system with respect to gravity. It is found that even a small amount of inclination (less than 10 deg) significantly lowers the critical Rayleigh number and moves the freckles to the sidewall of the casting, where the mushy zone has advanced the most relative to gravity. The critical Rayleigh number decreases further with increasing inclination. The predicted results on the inclination effect still need to be verified experimentally.

In application of the proposed Rayleigh number based freckle predictor to complex-shaped superalloy castings, the local thermal conditions, solidification path, and liquid densities need to be carefully evaluated. Also, the absence of freckles near upper and lower boundaries and in sections of insufficient cross-sectional area or height needs to be taken into account. These observations are consistent with the fact that the Rayleigh number criterion alone is not a sufficient condition for freckles to form.

Finally, it should be kept in mind that stability analyses have shown that the critical Rayleigh number varies with parameters such as the latent heat, the superheat, and the phase diagram.[3] Therefore, even if the variation of the permeability with solid fraction (Eq. [3]) is fairly universal, it is unclear if the present value of the critical Rayleigh number applies to the many freckling experiments that have been conducted using transparent model alloys and Pb-Sn alloys. This issue will be investigated in the near future.

ACKNOWLEDGMENTS

This work was supported, in part, by the Defense Advanced Research Project Agency (Agreement No. MDA972-93-2-0001), under the Micromodeling program of the Investment Casting Cooperative Arrangement (ICCA), through a subcontract to Howmet Corporation, and by the National Science Foundation (Grant No. CTS-9501389). The authors thank A.F. Giamei, UTRC, and other members of the ICCA consortium for fruitful discussions.

REFERENCES

1. R.J. McDonald and J.D. Hunt: *TMS-AIME*, 1969, vol. 245, pp. 1993-97.
2. A.F. Giamei and B.H. Kear: *Metall. Trans.*, 1970, vol. 1, pp. 2185-92.
3. M.G. Worster: *Ann. Rev. Fluid Mech.*, 1997, vol. 29, pp. 91-122.
4. A. Hellawell, J.R. Sarazin, and R.S. Steube: *Phil. Trans. R. Soc. London A*, 1993, vol. 345, pp. 507-44.
5. T.M. Pollock and W.H. Murphy: *Metall. Mater. Trans. A*, 1996, vol. 27A, pp. 1081-94.
6. J.P. Gu, C. Beckermann, and A.F. Giamei: *Metall. Mater. Trans. A*, 1997, vol. 28A, pp. 1533-42.
7. S.M. Copley, A.F. Giamei, S.M. Johnson, and M.F. Hornbecker: *Metall. Trans.*, 1970, vol. 1, pp. 2193-2204.
8. A.K. Sample and A. Hellawell: *Metall. Trans. A*, 1984, vol. 15A, pp. 2163-73.
9. J.R. Sarazin and A. Hellawell: *Metall. Trans. A*, 1988, vol. 19A, pp. 1861-71.
10. S.N. Tewari and R. Shah: *Metall. Trans. A*, 1992, vol. 23A, pp. 3383-92.
11. S.N. Tewari, R. Shah, and M.A. Chopra: *Metall. Trans. A*, 1993, vol. 24A, pp. 1661-69.
12. S.N. Tewari and R. Shah: *Metall. Mater. Trans. A*, 1996, vol. 27A, pp. 1353-62.
13. M.I. Bergman, D.R. Fearn, J. Bloxham, and M.C. Shannon: *Metall. Mater. Trans. A*, 1997, vol. 28A, pp. 859-66.
14. P. Auburtin, S.L. Cockcroft, and A. Mitchell: in *Solidification Processing 1997*, J. Beech and H. Jones, eds., The University of Sheffield, Sheffield, United Kingdom, 1997, pp. 336-40.
15. W. Kurz and D.J. Fisher: *Fundamentals of Solidification*, Trans Tech Publications, Aedermannsdorf, Switzerland, 1998.
16. P.N. Quested and M. McLean: *Mater. Sci. Eng.*, 1984, vol. 65, pp. 171-84.
17. G.K. Bouse and J.R. Mihalisin: in *Superalloys, Supercomposites and Superceramics*, J.K. Tien and T. Caulfield, eds., Academic Press, Boston, MA, 1988, pp. 99-148.
18. S. Tait and C. Jaupart: *J. Geophys. Res.*, 1992, vol. 97, pp. 6735-56.
19. A.C. Fowler: *IMA J. Appl. Math.*, 1985, vol. 35, pp. 159-74.
20. P. Nandapurkar, D.R. Poirier, J.C. Heinrich, and S. Felicelli: *Metall. Trans. B*, 1989, vol. 20B, pp. 711-21.
21. M.G. Worster: *J. Fluid Mech.*, 1992, vol. 237, pp. 649-69.
22. G. Amberg and G.M. Homsy: *J. Fluid Mech.*, 1993, vol. 252, pp. 79-98.
23. D.M. Anderson and M.G. Worster: *J. Fluid Mech.*, 1995, vol. 302, pp. 307-31.
24. W.D. Bennon and F.P. Incropera: *Int. J. Heat Mass Transfer*, 1987, vol. 30, pp. 2161-70.
25. C. Beckermann and C.Y. Wang: in *Annual Review of Heat Transfer VI*, C.L. Tien, ed., Begell House, New York, NY, 1995, vol. 6, pp. 115-98.
26. P.J. Prescott and F.P. Incropera: in *Advances in Heat Transfer*, D. Poulikakos, ed., Academic Press, San Diego, CA, 1996, pp. 231-338.

27. M.C. Schneider, J.P. Gu, C. Beckermann, W.J. Boettinger, and U.R. Kattner: *Metall. Mater. Trans. A*, 1997, vol, 28A, pp. 1517-31.
28. W.J. Boettinger, U.R. Kattner, S.R. Coriell, Y.A. Chang, and B.A. Mueller: in *Modeling of Casting, Welding and Advanced Solidification Process VII*, M. Cross and J. Campbell, eds., TMS, Warrendale, PA, 1995, pp. 649-56.
29. S.D. Felicelli, D.R. Poirier, and J.C. Heinrich: *Metall. Mater. Trans. A*, 1998, vol. 29A, pp. 847-55.
30. B. Mueller: Howmet Corporation, Whitehall, MI, personal communication, 1995.
31. M.C. Bhat: Ph.D. Thesis, The University of Arizona, Tucson, AR, 1995.
32. J.P. Gu and C. Beckermann: *Metall. Mater. Trans. A*, 1999, vol. 30A, pp. 1357-66.
33. T.G. Chart, J.F. Counsell, W. Slough, and P.J. Spencer: *Int. Met. Rev.*, 1975, vol. 20, p. 57.
34. U.R. Kattner, W.J. Boettinger, and S.R. Coriell: *Z. Metallkd.*, 1996, vol. 87, pp. 522-28.
35. T. Iida and R.I.L. Guthrie: in *The Physical Properties of Liquid Metals*, Clarendon Press, Oxford, United Kingdom, 1993, pp. 70-73.